Ultrathin Fe$_3$O$_4$ epitaxial films on wide bandgap GaN(0001)

P. K. J. Wong,[1,*] W. Zhang,[1] X. G. Cui,[2] Y. B. Xu,[1,†] J. Wu,[3] Z. K. Tao,[2] X. Li,[2] Z. L. Xie,[2] R. Zhang,[2] and G. van der Laan[4]

[1]*Spintronics and Nanodevice Laboratory, Department of Electronics, University of York, York YO10 5DD, United Kingdom*
[2]*Jiangsu Provincial Key Laboratory of Advanced Photonic and Electronic Materials and Department of Physics, Nanjing University, Nanjing 210093, People's Republic of China*
[3]*Department of Physics, University of York, York, YO10 5DD, United Kingdom*
[4]*Diamond Light Source, Chilton, Didcot OX11 0DE, United Kingdom*

Ultrathin films of magnetite (Fe$_3$O$_4$) have been grown epitaxially on wurtzite wide bandgap semiconductor GaN(0001) surfaces using molecular-beam epitaxy. Reflection high-energy electron-diffraction patterns show a (111) orientation of the Fe$_3$O$_4$ films and in-plane epitaxial relationship of $\langle 1\bar{1}0 \rangle_{Fe_3O_4} \| \langle 11\bar{2}0 \rangle_{GaN}$ and $\langle 11\bar{2} \rangle_{Fe_3O_4} \| \langle 1\bar{1}00 \rangle_{GaN}$ with the GaN(0001). X-ray photoelectron spectroscopy and x-ray magnetic circular dichroism confirm the growth of stoichiometric Fe$_3$O$_4$, instead of γ-Fe$_2$O$_3$. The magnetic hysteresis loops and saturation magnetization M_s obtained by superconducting quantum interference device at room temperature show fast saturation of the Fe$_3$O$_4$ films with the magnetization close to that of the bulk single-crystal value. In-plane magnetoresistance (MR) measurements reveal negligibly small MR effects, further indicating that the films are free from antiphase boundaries.

PACS number(s): 75.70.−i, 85.75.−d

I. INTRODUCTION

One of the major challenges in developing next generation spintronic devices, which integrate spin with semiconductors, is the synthesis of high quality magnetic materials with Curie temperatures (T_C) above room temperature (RT), large spin polarization at the Fermi level (E_F), and matched impedance between magnetic and semiconductor materials.[1,2] Among the wide range of magnetic materials including ferromagnetic transition metals, dilute magnetic semiconductors,[3,4] Heusler alloys,[5,6] and half-metallic magnetic oxides,[7] a highly relevant candidate perfectly matching the above criteria is Fe$_3$O$_4$. Half-metallic Fe$_3$O$_4$ is of great current interest as a RT spin injector due to its predicted half-metallicity,[8] strong measured spin polarization approaching 100% at E_F,[9] and high T_C of 858 K, well in excess of RT. To date, epitaxial growth of Fe$_3$O$_4$ films on a variety of conventional semiconductors, such as GaAs,[10,11] InAs,[12] and Si,[13] has been achieved, whereas possible growth on wide bandgap semiconductors, such as GaN, a technologically important material for fabrication of optoelectronic devices,[14,15] and high power transistors,[16] remains essentially unexplored. Recent GaN-based spin relaxation measurements yield spin lifetimes of ~20 ns at 5 K.[17] Theoretical calculations predicted that the spin lifetime in pure GaN is about three orders of magnitude larger than in GaAs for all temperatures.[18] These encouraging reports indicate that the inherent ability of GaN to sustain a long spin lifetime is greatly beneficial to device fabrication where spin transport at large length scales is required. It is, therefore, anticipated that the combination of half-metallic Fe$_3$O$_4$ and wide bandgap GaN could be one of the most promising magnetic-semiconductor hybrid systems for development of future spintronic devices.

Fe$_3$O$_4$ is a mixed-valence 3d transition-metal oxide that has an inverse spinel structure with a lattice constant of 8.397 Å. The tetrahedral sites of the spinel structure are en-

tirely occupied by Fe^{3+}, whereas the octahedral sites are occupied by both Fe^{2+} and Fe^{3+} cations. For heteroepitaxy of Fe$_3$O$_4$ on wurtzite GaN(0001), the {111} faces of Fe$_3$O$_4$ offers the best atomic registry. Figure 1 depicts schematically two possible atomic arrangements with each rotated 30° to the other, assuming that the Fe$_3$O$_4$(111) film is stabilized on the (0001) plane of GaN in a hexagon-on-hexagon manner. In terms of lattice matching, configuration (1) in Fig. 1(b), i.e., Fe$_3$O$_4$(111)$\langle 1\bar{1}0 \rangle$‖GaN(0001)$\langle 11\bar{2}0 \rangle$, gives a mismatch of −6.5% along $\langle 11\bar{2}0 \rangle$ and $\langle 1\bar{1}00 \rangle$ directions of GaN(0001), whereas −19.1% and 7.9% for configuration (2), with Fe$_3$O$_4$(111)$\langle 11\bar{2} \rangle$‖GaN(0001)$\langle 11\bar{2}0 \rangle$, given the lattice constants of Fe$_3$O$_4$ ($a_{Fe_3O_4}$) and GaN (a_{GaN}), are 8.396 and 3.189 Å,[19] respectively. In accordance, it is predicted that the former provides a crystallographically more favorable arrangement of the heterostructure.

In this work, we have investigated the epitaxial growth of Fe$_3$O$_4$ ultrathin films on GaN(0001) by molecular-beam epitaxy (MBE). The structural and magnetic properties of this
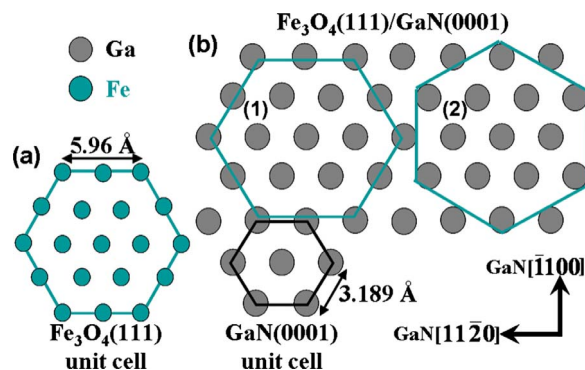

FIG. 1. (Color online) The unit cell of Fe$_3$O$_4$(111) and GaN(0001) is shown, respectively, in (a) and (b). Two possible atomic arrangements of Fe$_3$O$_4$(111) on GaN(0001) are also schematically depicted in (b).
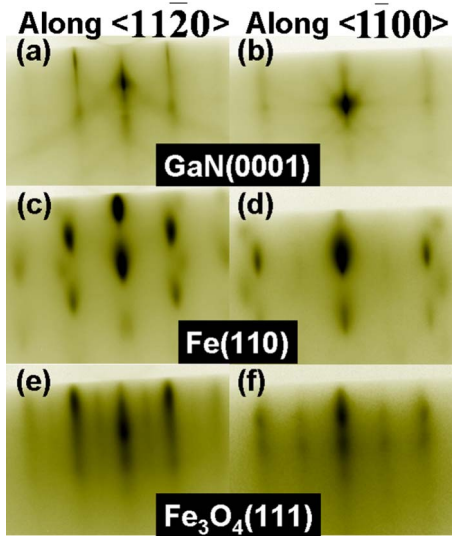
FIG. 2. (Color online) RHEED patterns taken from the GaN(0001) substrate, Fe(110), and Fe_3O_4(111) layers with a beam energy of 10 kV: (a) and (b) GaN surface after *in situ* annealing; (c)–(d) after growth of Fe(110) at RT; (e)–(f) after oxidation of Fe(110).

new hybrid material have been thoroughly studied by reflection high-energy electron diffraction (RHEED), x-ray photoelectron spectroscopy (XPS), x-ray magnetic circular dichroism (XMCD), superconducting quantum interference device (SQUID), and magnetoresistance (MR) measurements. To our knowledge, there have been no previous reports of single-crystal Fe_3O_4 growth on GaN and the present work can have an impact on developing and understanding this class of hybrid spintronic structure.

II. EXPERIMENTAL DETAILS

The 2 μm thick GaN films used in this study have been prepared by metal-organic chemical vapor deposition with a 20 nm low-temperature grown buffer layer on sapphire. Prior to the growth of the magnetic materials, the GaN surface was exposed to a 1:1 $HCl:H_2O$ solution, followed by a 1:99 $HF:H_2O$ solution for 2 min each with de-ionized water rinse between and after etching.[20] Once loaded into the chamber, the substrates were annealed at 600 °C for 1 h. Figures 2(a) and 2(b) shows the RHEED patterns of a GaN(0001) surface just after annealing followed by cooling to RT for subsequent Fe growth. The streaky (1×1) patterns with clear Kikuchi lines suggest a smooth GaN surface. Fe films of a thickness t_{Fe} ranging from 3.0 to 6.0 nm were deposited by *e*-beam evaporation at RT at a rate of 2 Å/min, and then oxidized to Fe_3O_4 by exposure to high-purity oxygen gas at an O_2 partial pressure of 8×10^{-4} mbar at 230 °C for 10 min.[10] After growth, the samples were retrieved from the growth chamber without a capping layer for subsequent *ex situ* characterizations. Thereafter, the nominal thicknesses of the predeposited Fe layers were quoted for the samples after the oxidation.

III. RESULTS AND DISCUSSION

The RHEED patterns along different azimuths for a 5.0 nm Fe layer are shown in Figs. 2(c) and 2(d) and for the
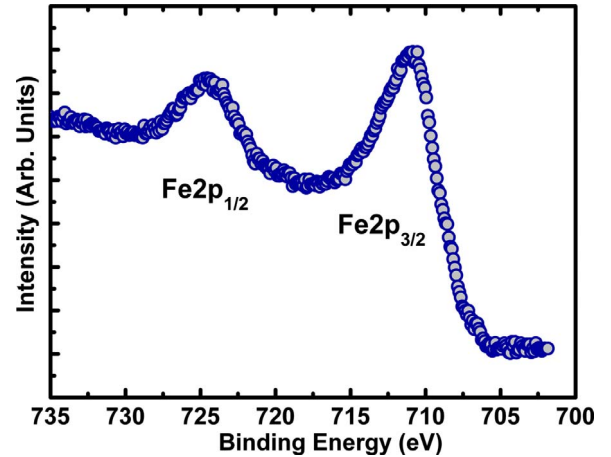

FIG. 3. (Color online) Fe $2p$ core-level XPS spectrum obtained with normal incidence with respect to the surface of a 5.0 nm oxidized film using Mg $K\alpha$ radiation.

oxidized layer in Figs. 2(e) and 2(f). The RHEED patterns of the Fe layer consist of a set of less intense reflections besides the main streaks of Fe. We attribute these features in the patterns to the formation of epitaxial domains of bcc Fe(110) with three different orientations on the hexagonal GaN substrates. This is similar to that reported for Fe/Al_2O_3(0001) by Shiratsuchi *et al.*[21] The epitaxial relationship of the Fe film and GaN substrate as shown by the angular variation in the RHEED patterns in Figs. 2(c) and 2(d) is $(110)_{Fe}\|(0001)_{GaN}$ and $\langle 001 \rangle_{Fe}\|\langle 11\bar{2}0 \rangle_{GaN}$ with the Fe in bcc structure. Upon oxidation of the Fe films, both half- and first-order type streaks are present in Figs. 2(e) and 2(f), which are the characteristic patterns for the inverse spinel structure of Fe_3O_4. Comparing Figs. 2(e) and 2(f) with Figs. 1(a) and 1(b), the in-plane symmetries of the Fe_3O_4 layer are clearly the same as those of the GaN(0001) substrate and no rotation of the Fe_3O_4 lattice cell with respect to that of the GaN is observed. The intensity profile of the RHEED patterns gives an in-plane lattice-parameter $a_{Fe_3O_4}$ of 6.10 Å for the Fe_3O_4 layer. This value matches well with the bulk Fe_3O_4(111) value $a_{bulk}=5.96$ Å.[22] We thus have an epitaxial Fe_3O_4 film with [111] axis perpendicular to the GaN(0001) surface and with epitaxial relationships $Fe_3O_4(111)\langle 1\bar{1}0 \rangle\|GaN(0001)\langle 11\bar{2}0 \rangle$ and $Fe_3O_4(111)\langle 11\bar{2} \rangle\|GaN(0001)\langle 1\bar{1}00 \rangle$, supporting our inferred atomic configuration (1) of Fig. 1(b).

One also needs to consider the possible existence of a metastable iron oxide phase γ-Fe_2O_3, which has almost the same inverse spinel structure as that of Fe_3O_4. It is, in practice, difficult to distinguish the two phases by RHEED patterns, which prompted us to characterize the films using XPS, probing the Fe valence state rather than its crystal structure. Figure 3 shows the Fe $2p$ core-level spectrum of a 5.0 nm sample obtained at normal incidence with respect to the film surface using Mg $K\alpha$ radiation. It is well established that peak positions and satellite structures in the XPS spectra are reliable means for identifying the state of Fe oxidation. From the figure, it is evidenced that the Fe $2p_{3/2}$ and Fe $2p_{1/2}$ peaks situated at around 711 and 724 eV between which a
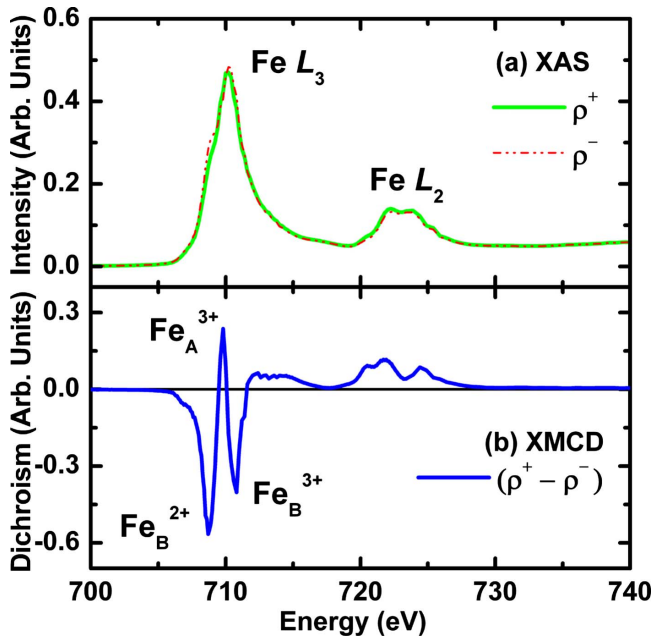
FIG. 4. (Color online) (a) Fe $L_{2,3}$ edge XAS and (b) XMCD spectra of a 5.0 nm Fe_3O_4/GaN(0001) ultrathin film measured at RT. The labels A and B denote tetrahedral and octahedral sites, respectively, of the Fe ions.
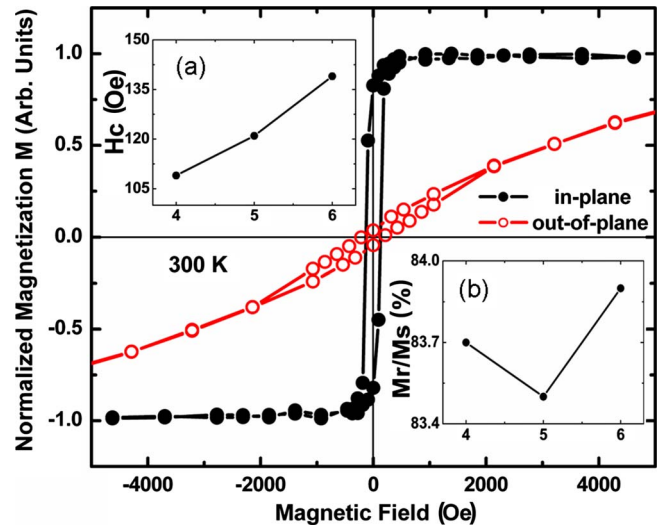

FIG. 5. (Color online) SQUID measurements of 5.0 nm Fe_3O_4/GaN(0001) at RT. The magnetic field was applied along the $[1\bar{1}00]$ direction of the GaN film for the in-plane measurements. Inset (a) and (b) show, respectively, the thickness dependent coercivity and squareness of the hysteresis loop of the magnetite films. The x axis of both insets represents the Fe thickness in nm. The predetermined diamagnetic signals of the sapphire substrates have been subtracted from the data.

board and structureless region can be identified, therefore suggesting the coexistence of the Fe^{3+} and Fe^{2+} cations.[23,24] More importantly, no satellite can be identified at a binding energy of ~719 eV, further eliminating the possible formation of γ-Fe_2O_3.[25]

We performed x-ray absorption spectroscopy (XAS) and XMCD measurements to further characterize the magnetite films. Figure 4 shows the Fe $L_{2,3}$ XAS and XMCD spectra of Fe_3O_4/GaN(0001) with t_{Fe}=5.0 nm taken at RT. The measurements, in total electron yield mode using circularly polarized x-rays, were performed in a portable octupole magnetic system at station 5U.1 of the Synchrotron Radiation Source at Daresbury Laboratory, U.K. The XMCD is the difference between the XAS spectra measured with a 0.6 T magnetic field applied parallel and antiparallel to the incident x-ray beam. The characteristic ferrimagnetic multiplet structure of the Fe $L_{2,3}$ XAS and XMCD spectra, which features contributions from both Fe^{3+} cations at tetrahedral sites and Fe^{2+} and Fe^{3+} cations at octahedral sites, shows a good agreement with stoichiometric Fe_3O_4 [26,27] and, accordingly, provides direct evidence for the formation of Fe_3O_4 with a quality close to that of the bulk. It should be noted that, in the case of γ-Fe_2O_3, the peak corresponding to octahedral Fe^{2+} would be strongly suppressed.[28,29]

Magnetic hysteresis loops of the magnetite films measured by SQUID in the in-plane and out-of-plane geometry are depicted in Fig. 5. The external applied field was applied along the $[1\bar{1}00]$ axis in-plane and along the [0001] axis out-of-plane of the GaN film. All the films exhibit an easy in-plane magnetization due to the presence of shape anisotropy of the thin films. Also notable in the figure is the saturation of magnetization M_s of the 5.0 nm sample at a field strength of ~470 Oe. The coercivity H_c of the Fe_3O_4 film

increases with increasing t_{Fe} as shown in inset (a) of Fig. 5; while in inset (b), the squareness, which is defined as M_r/M_s remains fairly high and is largely constant within the range of t_{Fe} examined, indicating a good degree of magnetic ordering inside the films. The fast saturation behavior in our films is in contrast to the high-field magnetization slope observed in Fe_3O_4 films grown on MgO, in which the epitaxial films are known to possess a high density of antiphase boundaries (APBs), thereby leading to an unsaturated magnetization at magnetic fields as high as ~70 kOe.[30] This suggests that the Fe_3O_4 films in the present study might be free from APBs or have a low density of such defects as we found previously in Fe_3O_4/GaAs(100) system.[10]

In order to gain insight into this issue, in-plane MR measurements of the magnetite films were performed in a standard four-probe configuration at RT. Electrical Ohmic contacts to the Fe_3O_4 films were made of thermally evaporated 50 nm Au buffered with 10 nm Cr into which the current that is along the $[1\bar{1}00]$ direction of the GaN(0001) was applied. Such characterizations are reminiscences of the work delivered by Ziese and Blythe, in which the authors compared bulk and thin-film MR of Fe_3O_4.[31] Strikingly, they found abnormal electrical properties manifested as the high-field MR in the epitaxial films on MgO, in contrast with the negligible MR in the bulk. This remarkable discrepancy has been attributed to the drastic alterations in electron transport in the Fe_3O_4 films with the APBs.[31] Having recalled the above relevant report, we show in Fig. 6 the MR of a 4.0 nm oxidized film, from which a clear anisotropic MR with the film resistance in the longitudinal direction increases and saturates to a constant value above the saturation field when the magnetization is aligned with the external field is re-
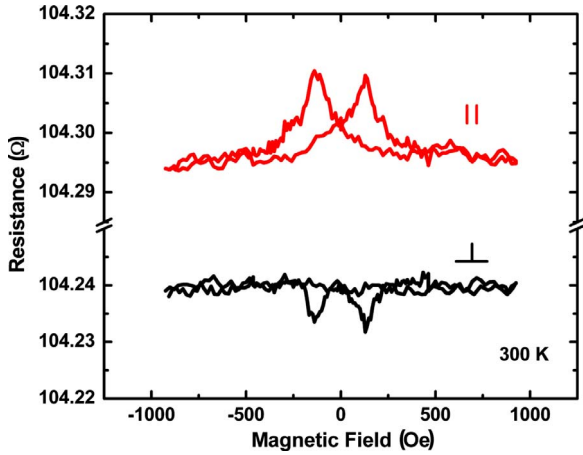
FIG. 6. (Color online) Longitudinal (upper curve) and transverse (lower curve) MR measurements of a 4.0 nm oxidized film acquired at RT. The applied current was along $[1\bar{1}00]$ crystallographic direction of GaN(0001).

vealed; The opposite is observed in the transverse geometry. Here, the MR is defined as $(R_{Hc}-R_H)/R_H$ where R_H and R_{Hc} denote, respectively, the resistance at 900 Oe and at the H_c of the film. The MR changes in the two geometries are, respectively, 0.0137% and −0.0069%. Notice that other film thicknesses also exhibit comparably small MR values, consistent with the very small MR effect of the Fe_3O_4 single crystal as mentioned. At this point, both SQUID and MR data support the hypothesis of a limited density of APBs in our oxide films. In particular, the latter results we have here are not in line with a belief of several former publications on reduced APB density in thicker magnetite films due to the larger Fe_3O_4 grain sizes that formed.[32,33]

The values of M_s of the magnetite films with t_{Fe} spanning from 3.0 to 6.0 nm have also been extracted from the SQUID data and are shown in Fig. 7. The M_s approaches that of the single-crystal value of 477 emu cm^{-3} with the thickness above 5.0 nm.[34] Considering the evolution of the M_s with t_{Fe}, we suggest that residual strain in the oxidized films may play a role in the M_s reduction in the thinner films. It is arguable that the lowered values might be associated with parasitic phases like α-Fe_2O_3 and FeO, since the information depth by the x-ray techniques used in this study did not probe the entire films. However, this appears unlikely because the presence of these phases should have altered the XMCD spectrum, as reported by Lu *et al.*[35] The present discussion can be, therefore, narrowed to either a Fe_3O_4-GaN interface- or a strain-driven or both M_s reduction mechanisms in the magnetic films with t_{Fe} less than 5.0 nm, which is interesting for further investigations in the future.
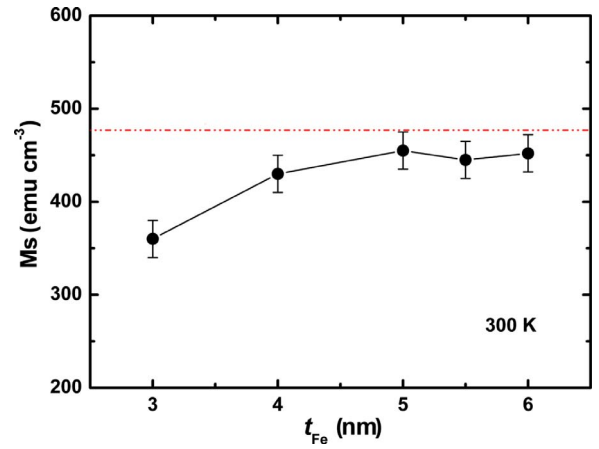

FIG. 7. (Color online) Thickness dependence of saturation magnetization M_s of Fe_3O_4/GaN(0001) determined by SQUID at RT. The dotted line indicates the single-crystal value of 477 emu cm^{-3} (Ref. 34).

IV. CONCLUSIONS

In summary, we have demonstrated the epitaxial growth of single-crystal ultrathin Fe_3O_4(111) films on wide bandgap semiconductor GaN(0001) by postgrowth annealing of epitaxial ultrathin Fe films in an oxygen environment. The Fe_3O_4 unit cell shows no rotation with respect to that of the GaN substrate despite the 6.5% lattice mismatch. XAS and XMCD results reveal the characteristic ferrimagnetic coupling in Fe_3O_4. XPS and XMCD results eliminate the possible formation of metastable phase γ-Fe_2O_3. The fast saturation of the films at a field as low as 470 Oe shows that there is no evidence of APBs in our Fe_3O_4 thin films on GaN. This is further supported by the negligible MR values found in the magnetotransport measurements. The slight deviation of the saturation magnetization from that of the single-crystal counterpart has been ascribed to an interface-, or a strain-driven or both mechanisms. These results might represent a significant step toward the development of functional magnetic oxide spintronic materials operational at room temperature that integrate with the intriguing properties of GaN.

*Present address: MESA+ Institute for Nanotechnology, University of Twente, P.O. Box 217, 7500 AE Enschede, The Netherlands.
†yx2@ohm.york.ac.uk
[1] S. A. Wolf, D. D. Awschalom, R. A. Burham, J. M. Daughton, S. von Molnár, M. L. Roukes, A. Y. Chtchelkanova, and D. M. Treger, Science **294**, 1488 (2001).
[2] *Spintronic Materials and Technology*, edited by Y. B. Xu and S. M. Thompson (Taylor & Francis, London, 2006).
[3] T. Dietl, H. Ohno, F. Matsukura, J. Cibert, and D. Ferrand, Science **287**, 1019 (2000).

[4] S. A. Chambers and R. F. C. Farrow, MRS Bull. **28**, 729 (2003).

[5] R. A. de Groot, F. M. Mueller, P. G. van Engen, and K. H. J. Buschow, Phys. Rev. Lett. **50**, 2024 (1983).

[6] C. Palmstrøm, MRS Bull. **28**, 725 (2003).

[7] J. M. D. Coey and C. L. Chien, MRS Bull. **28**, 720 (2003).

[8] Z. Zhang and S. Satpathy, Phys. Rev. B **44**, 13319 (1991).

[9] Yu. S. Dedkov, U. Rüdiger, and G. Güntherodt, Phys. Rev. B **65**, 064417 (2002).

[10] Y. X. Lu, J. S. Claydon, Y. B. Xu, S. M. Thompson, K. Wilson, and G. van der Laan, Phys. Rev. B **70**, 233304 (2004).

[11] Y. B. Xu, E. Ahmad, J. S. Claydon, Y. X. Lu, S. S. A. Hassan, I. G. Will, and B. Cantor, J. Magn. Magn. Mater. **304**, 69 (2006).

[12] M. Ferhat and K. Yoh, Appl. Phys. Lett. **90**, 112501 (2007).

[13] R. J. Choudhary, S. Tiwari, D. M. Phase, R. Kumar, P. Thakur, K. H. Chae, and W. K. Choi, Appl. Phys. Lett. **92**, 072102 (2008).

[14] S. Nakamura, T. Mukai, and M. Senoh, Appl. Phys. Lett. **64**, 1687 (1994).

[15] S. Nakamura, M. Senoh, S. Nagahama, N. Iwasa, T. Yamada, T. Matsushita, H. Kiyoku, and Y. Sugimoto, Jpn. J. Appl. Phys. **35**, L74 (1996).

[16] U. K. Mishra, Y.-F. Wu, B. P. Keller, S. Keller, and S. P. Den-Baars, in *Physics of Semiconductor Devices*, edited by V. Kumar and S. K. Agarwal (India Norosa, Delhi, 1998), Vol. II, p. 878.

[17] B. Beschoten, E. Johnston-Halperin, D. K. Young, M. Poggio, J. E. Grimaldi, S. Keller, S. P. DenBaars, U. K. Mishra, E. L. Hu, and D. D. Awschalom, Phys. Rev. B **63**, 121202(R) (2001).

[18] S. Krishnamurthy, M. van Schilfgaarde, and N. Newman, Appl. Phys. Lett. **83**, 1761 (2003).

[19] M. Leszczynski, H. Teisseyre, T. Suski, I. Grzegory, M. Bockowski, J. Jun, S. Porowski, K. Pakula, J. M. Baranowski, C. T. Foxon, and T. S. Cheng, Appl. Phys. Lett. **69**, 73 (1996).

[20] L. L. Smith, S. W. King, R. J. Nemanich, and R. F. Davis, J. Electron. Mater. **25**, 805 (1996).

[21] Y. Shiratsuchi, Y. Endo, M. Yamamoto, and S. D. Bader, J. Appl. Phys. **97**, 10J106 (2005).

[22] C. N. Rao and B. Raveau, *Transitional Metal Oxides* (VCH, New York, 1995).

[23] C. Ruby, B. Humbert, and J. Fusy, Surf. Interface Anal. **29**, 377 (2000).

[24] T. Fujii, F. M. F. de Groot, G. A. Sawatzky, F. C. Voogt, T. Hibma, and K. Okada, Phys. Rev. B **59**, 3195 (1999).

[25] S. Gota, E. Guiot, M. Henriot, and M. Gautier-Soyer, Phys. Rev. B **60**, 14387 (1999).

[26] P. Morrall, F. Schedin, G. S. Case, M. F. Thomas, E. Dudzik, G. van der Laan, and G. Thornton, Phys. Rev. B **67**, 214408 (2003).

[27] D. J. Huang, C. F. Chang, H.-T. Jeng, G. Y. Guo, H.-J. Lin, W. B. Wu, H. C. Ku, A. Fujimori, Y. Takahashi, and C. T. Chen, Phys. Rev. Lett. **93**, 077204 (2004).

[28] L. Signorini, L. Pasquini, F. Boscherini, E. Bonetti, I. Letard, S. Brice-Profeta, and Ph. Sanctavit, Phys. Rev. B **74**, 014426 (2006).

[29] E. Pellegrain, M. Hagelstein, S. Doyle, H. O. Moser, J. Fuchs, D. Vollath, S. Schuppler, M. A. James, S. S. Saxena, L. Niesen, O. Rogojanu, G. A. Sawatzky, C. Ferrero, M. Borowski, O. Tjernberg, and N. B. Brookes, Phys. Status Solidi **215**, 797 (1999) b.

[30] D. T. Margulies, F. T. Parker, F. E. Spada, R. S. Goldman, J. Li, R. Sinclair, and A. E. Berkowitz, Phys. Rev. B **53**, 9175 (1996).

[31] M. Ziese and H. J. Blythe, J. Phys.: Condens. Matter **12**, 13 (2000).

[32] W. Eerenstein, T. T. M. Palstra, T. Hibma, and S. Celotto, Phys. Rev. B **66**, 201101 (2002).

[33] J.-B. Moussy, S. Gota, A. Bataille, M.-J. Guittet, M. Gautier-Soyer, F. Delille, B. Dieny, F. Ott, T. D. Doan, P. Warin, P. Bayle-Guillemaud, C. Gatel, and E. Snoeck, Phys. Rev. B **70**, 174448 (2004).

[34] S. Okamoto and K. Kohn, *Magnetic Ceramics* (Gihodo, Japan, 1986), p. 84.

[35] Y. X. Lu, J. S. Claydon, E. Ahmad, Y. B. Xu, S. M. Thompson, K. Wilson, and G. van der Laan, IEEE Trans. Magn. **41**, 2808 (2005).